Title	Evaluation of Atkin's model of ductile machining including the material separation component(Accepted version)
Author(s)	Subbiah, Sathyan; Melkote, Shreyes N.
Citation	Subbiah, S., & Melkote, S. N. (2007). Evaluation of Atkin's model of ductile machining including the material separation component. Journal of Materials Processing Technology, 182(1-3), 398-404.
Date	2007
URL	http://hdl.handle.net/10220/4511
Rights	© 2007 Elsevier This is the author created version of a work that has been peer reviewed and accepted for publication by Journal of Materials Processing Technology, Elsevier. It incorporates referee's comments but changes resulting from the publishing process, such as copyediting, structural formatting, may not be reflected in this document. The published version is available at: [DOI: http://dx.doi.org/10.1016/j.jmatprotec.2006.08.019]

Evaluation of Atkins' model of ductile machining including the material separation component

Sathyan Subbiah, Shreyes N. Melkote *

The George W. Woodruff School of Mechanical Engineering
Georgia Institute of Technology
813 Ferst Dr. NW
Atlanta, GA 30332, USA

Abstract

This paper provides data along with experimental evidence of ductile material separation that supports the Atkins' model of machining, which includes the energy needed for material separation along with shear and frictional dissipation. This model proposed earlier explicitly includes the energy needed for material separation in addition to that needed for shear and friction. However, no experimental evidence for material separation via ductile tearing or fracture was provided. In this work, orthogonal cutting is performed on oxygen-free high conductivity (OFHC) Copper, a highly ductile metal, at very low speeds and low uncut chip thickness where size-effect is observed. The chip-workpiece interface is observed under a scanning electron microscope to find evidence of material separation via ductile fracture. For values of fracture toughness and shear yield stress, that are of the same order of magnitude as that reported in the literature for OFHC Copper, the Atkins model captures the trend and the predictions are seen to be comparable to experimental data.

1 Introduction

Many researchers are investigating mechanical removal of material for manufacturing micro/meso scale parts (micro-cutting). For example, Yamagata et al. [1] have used the micro-cutting process to fabricate a vibration gyro in combination with a piezo film deposition process. They have reported that

* Corresponding author: Email: shreyes.melkote@me.gatech.edu; ph. +1-404-894-8499; fax: +1-404-894-9342

micro-cutting offers several advantages including capability to process several materials, to create three dimensional structures, and to provide good surface finish. As in other areas of engineering, scaling effects are present in cutting at the micro/meso scale (0.1-500 μm) as well. One such scaling effect is known as the size-effect in specific cutting energy. The specific cutting energy is the energy needed to remove a unit volume of material and is seen to increase non-linearly as the undeformed chip thickness is reduced to zero. Two approaches have been taken in the literature to explain the size-effect phenomenon in micro-cutting: one retains the traditional approach of energy expended in shear and friction alone while accounting for the size-effect phenomenon as a change in the energy expended in these two; the second approach explicitly accounts for other energy sinks.

In the former traditional approach, machining models developed for sharp cutting tools typically account for the energy consumed in machining via energies for shearing the metal and overcoming friction between the chip and tool [2]. The energy used to separate the chip from the metal just ahead of the cutting tool tip, historically accounted for using solid surface energy (tension), is considered negligible in comparison with that consumed in shear and friction [2, 3]. Additionally, the energy associated with momentum change as the metal crosses the shear plane has been shown to be negligible [3]. However, it has been mentioned by Merchant [2] that at very small uncut chip thickness values less than 0.254 μm the energy for material separation may become significant. Merchant also points out that upon considering the local plastic flow the energy required for material separation would be more, but would still be negligible in comparison to shear and friction. Analytic predictive models, following a similar modeling approach, have been largely unsuccessful in predicting the material dependence of the shear angle.

Relying on this traditional modeling approach, several researchers [4, 5, 6, 7, 8] have sought explanations for the size-effect in specific cutting energy by investigating why the energy expended in shear and friction could be more than expected at smaller uncut chip thickness values. These explanations range from increase in shear energy expended due to increase in material strength resulting from strain-rate increase [5], strain-gradient effects [9, 6, 10], lack of defects at small uncut chip thicknesses [11], cutting edge radius contribution to material flow [7] around the tool tip etc. Other explanations such as subsurface plastic flow [12] and pushing of the material by the tool [13], similar to a punch, have also been offered. This modeling approach of considering only the shear and friction energies expended in cutting has been unable to fully account for the observed phenomenon of the increase in specific cutting energy as the uncut chip thickness is reduced.

The second modeling approach accounts for a third energy sink. Since no tool is perfectly sharp, a corresponding force is said to act on the cutting edge.

This force is considered to not contribute to chip formation and is collectively called the ploughing force (see [14] for a review on ploughing forces). The energy spent in ploughing due to the finite edge radius has been attributed to the size effect [15]. Recently, a model that explicitly accounts for the energy consumed in material separation as the third energy sink has been proposed by Atkins [16, 17]. In his earlier work, Atkins [16] presented a metal cutting theory for brittle materials that incorporates fracture. Fracture is considered to be the mechanism of material separation leading to chip formation. In subsequent work [17], Atkins argued that ductile fracture mechanics can be used to explain chip formation in ductile metals by incorporating fracture toughness as the specific work of surface creation into the machining model in addition to energy expended in shear and friction. This provides a constant term in the force expression that gives rise to the size-effect. This approach was also shown to account for the observed trends in shear angles with decrease in uncut chip thickness. Atkins has also suggested this as a way to establish fracture toughness values of materials [18]. However, Atkins provided no direct evidence of ductile fracture as the cause for chip formation.

This paper follows the Atkins approach and tests the model at cutting conditions where strain-rate, and temperature effects are low. Evidence of ductile tearing as the cause of material separation is provided in the form of scanning electron micrographs of the chip-workpiece interface at small uncut chip thickness where the size-effect is observed. The Atkins model is seen to apply well, and captures trends, for values of fracture toughness, coefficient of friction and shear yield stress, that are within an order of magnitude of that reported in the literature for OFHC Cu.

2 Atkins model

Atkins [17] argued the applicability of modern ductile fracture mechanics in modeling the cutting process. He cites the work associated with the chip separation criterion in Finite Element simulations of machining to be orders of magnitude different from that associated with chemical surface energy or solid surface tension, and comparable to fracture toughness values. The work done in cutting is accounted for by: (a) plasticity along the shear plane, (b) friction at the tool-chip interface, and (c) formation of new surfaces. This results in the following equation [17] for the cutting power:

$$F_c V = (\tau_y \gamma)(t_o w V) + [F_c \sec(\beta - \alpha) \sin\beta] \frac{V \sin\phi}{\cos\phi - \alpha} + RwV, \tag{1}$$

where the last term represents the energy involved in the formation of the new surface. R is the specific work of surface formation (fracture toughness), w, the

width of cut, τ_y, the shear yield stress, β, the friction angle, α, the rake angle, t_o, the uncut chip thickness, F_c, the cutting force, and V, the cutting speed. The energy terms are also illustrated in Fig. 1. It can be seen from Eq. 1 that

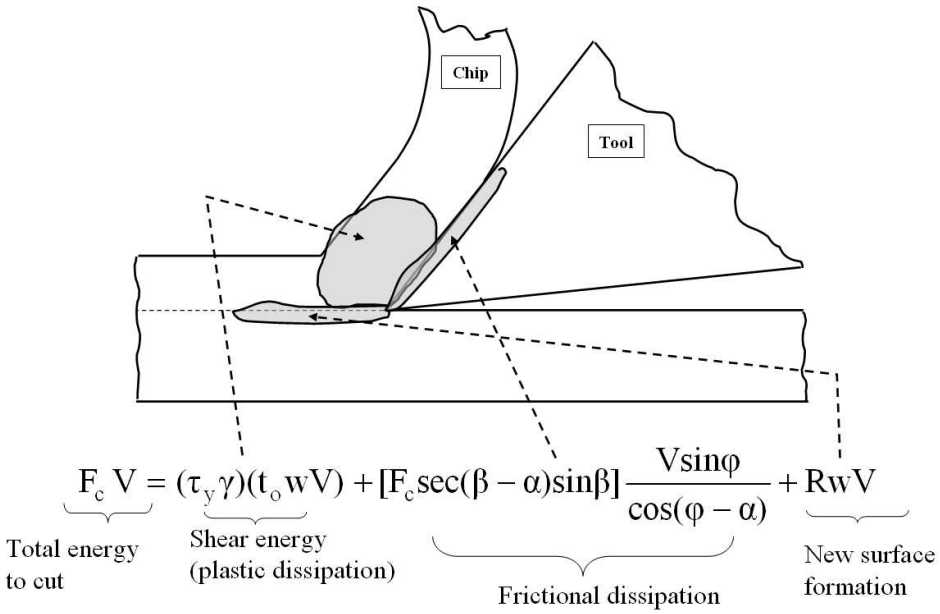

Fig. 1. Distribution of energy in cutting

if the other components of energy can be ignored, then for a unit width of cut, the fracture energy term naturally gives rise to a constant component of the cutting force viz., R. When Atkins applied this theory to data in the literature, the values of R needed to get a good fit of data were, in some workpiece materials, an order of magnitude lower than that obtained using standard fracture tests [17]. The reason attributed to this was as follows: machining involves high strains, strain-rates and temperatures, conditions which can alter the fracture toughness of metals.

Based on this argument, at cutting conditions where strain-rate, and temperature effects are low, the values of fracture toughness needed for the model should be comparable to that seen in the fracture mechanics literature. This would then confirm the applicability of the model. Strain-rates and temperature effects are minimal at very low cutting speeds. Under conditions of high rake angles and low cutting speeds, the authors [19] have reported the presence of a constant force component [20] and have shown evidence of ductile tearing ahead of the tool. However, due to experimental limitations, experiments were performed at higher uncut chip thickness values where the size-effect may not be prominent. In this work, experiments are performed at lower uncut chip thickness values to confirm if indeed Atkins' model captures the size-effect.

Table 1
Nominal composition of OFHC Copper (weight %)

OFHC-Cu
Cu 99.99%
Pb 0.001%
Zn 0.0001%
P 0.0003%

3 Experimental Conditions

A simple orthogonal tube cutting operation was performed on a Hardinge T42SP super precision lathe. Wedge shaped cutting tools were made from M2 grade high speed steel (HSS) blanks (Fig. 2). The necessary geometry of the cutting edge was carved out of the HSS blank using the wire-EDM process. The tool has a fixed clearance angle of 5^o. Lower clearance angles resulted in poor cutting action. The workpiece material was oxygen free high

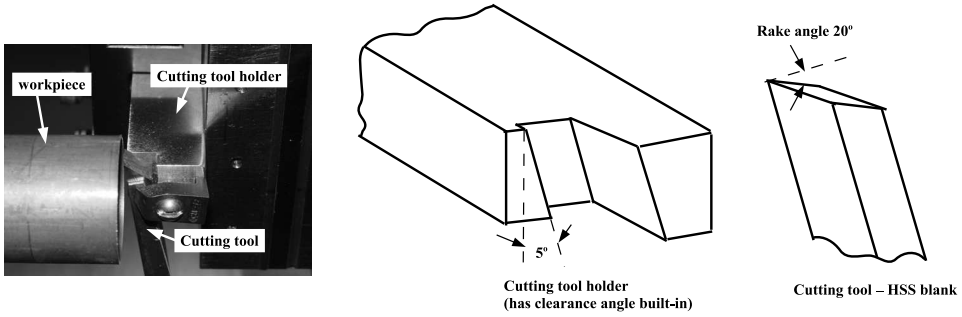

Fig. 2. Setup for performing experiments

conductivity (OFHC) copper. The nominal composition of OFHC copper is given in Table 1. The outer diameter of OFHC Copper tube was 38.1 mm and 1.1 mm thick. OFHC copper is almost pure Copper, is very ductile, has documented properties of fracture toughness [21], and is a relatively simple material for analytical modeling. A quartz 3-component Kistler dynamometer (Type 9257B) was used to measure the cutting forces. Table 2 summarizes the experimental conditions. The tool edge radius was measured using an SEM (Fig. 3) and determined to be $\sim 7\mu m$. Note that the smallest uncut chip thickness is twice the edge radius, thus minimizing edge radius effects on the measured forces. The chip thickness was measured at three different places along the length of the chip using a micrometer with a least count of $2.5\mu m$. All experiments were repeated thrice. At DOC=$25\mu m$ and $50\mu m$, the cutting was suddenly stopped in the middle of the cut to obtain the chip-workpiece interface. This interface was then observed in an SEM. The lowest rake angle at which chip formation was observed was 30^o at a cutting speed of 1.2 m/min.

Table 2
Experimental Conditions

Workpiece	OFHC Copper (38.1 mm diameter tube)
Tool	HSS M2 grade
Rake angle	30^o
Cutting speed	1.2 m/min (10 RPM Spindle Speed)
t_o	75-200 μm
Cut width	1.1 mm
Edge radius	$\sim 7\mu m$

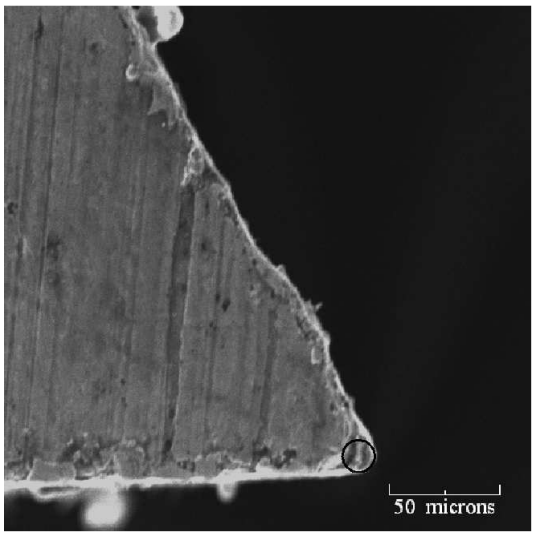

Fig. 3. Edge radius measured using an SEM

4 Experimental Results

4.1 Force and chip thickness

The experimental results are shown in Table 3. The table gives the average values of the cutting force (F_c) and its standard deviation σ_{F_c}, thrust force (F_t) and its standard deviation σ_{F_t}, and chip thickness (t_c) and its standard deviation σ_{t_c}. Also shown is the calculated specific cutting energy U along with its standard deviation σ_U, and the coefficient of friction calculated from the measured forces. The size-effect can be clearly seen in the specific cutting energy values with decrease in the uncut chip thickness (see also Fig. 8). The coefficient of friction is also seen to increase as t_o decreases.

Table 3
Experimental Results

t_o (μm)	F_c (N)	σ_{F_c} (N)	F_t (N)	σ_{F_t} (N)	t_c (mm)	σ_{t_c} (mm)	U (MPa)	σ_U (MPa)	μ
15	21.06	1.98	13.06	1.37	0.043	0.006	1207.04	119.82	1.08
25	24.99	2.91	14.33	2.36	0.057	0.006	854.32	105.78	1.04
35	30.13	2.28	16.01	2.31	0.066	0.006	753.17	59.21	1.01
50	37.8	0.63	16.87	0.31	0.086	0.004	680.72	11.44	0.94
60	41.63	0.92	16.58	0.75	0.099	0.004	635.45	13.91	0.90
70	48.04	0.41	18.26	0.58	0.119	0.007	623.14	5.34	0.89

4.2 Evidence of ductile tearing

To confirm that ductile tearing is indeed occurring at the chip-workpiece interface ahead of the tool, the interface was observed in an SEM for the two cases of $25\mu m$ and $50\mu m$ uncut chip thickness. The results are shown in Figs. 4 and 5. Each figure has three images with increasing magnification from left to right.

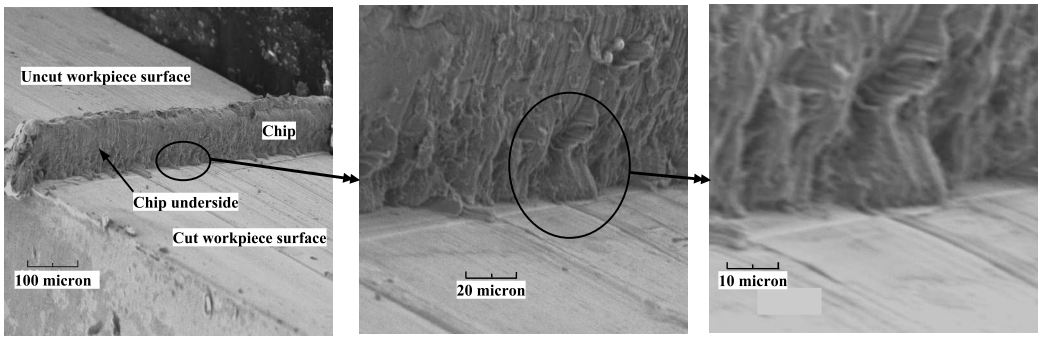

Fig. 4. SEM images of chip-workpiece interface for t_o=25μm

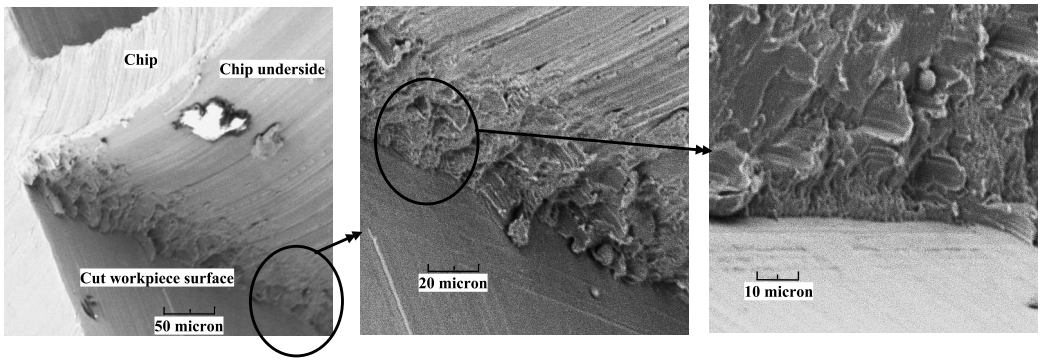

Fig. 5. SEM images of chip-workpiece interface for t_o=50μm

Some evidence of strands of copper attached to the underside of the chip and the newly formed machined surface can be seen. OFHC copper is known to fail in a ductile manner by void formation and coalescence [22]. The strands at the interface suggest a failure by ductile tearing leading to chip formation [23]. Ductile fracture through void formation and void growth is illustrated in Fig. 6. Plastic extension causes voids to enlarge, leading to material between voids to

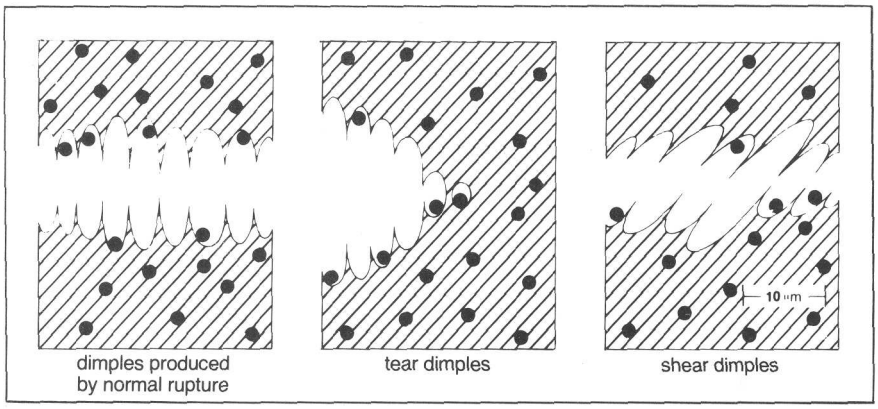

Fig. 6. Illustration of ductile tearing by void growth [23]

neck down, resulting in adjacent material being subjected to intense shearing [23]. Eventually, with continued extension, all that remains are thin ridges marking the separation between the holes. The strands seen in Figs. 4 and 5 are such thin ridges about to be separated.

5 Fitting Atkins Model

Atkins' machining model explicitly accounts for energies expended in shear, friction and material separation as shown in Eq. 1. While, the experimental shear angle ϕ_E is calculated from the measured chip thickness value as,

$$\phi_E = tan^{-1}\left(\frac{t_o \cos\alpha}{t_c - t_o \sin\alpha}\right) \tag{2}$$

and the shear angle ϕ_M, according to Merchant's model (obtained by minimizing only the first two terms of Eqn. 1), is calculated as,

$$\phi_M = \frac{\pi}{4} - \frac{1}{2}(\beta - \alpha) \tag{3}$$

the shear angle, according to Atkins' model, is calculated by numerically solving the following equation obtained by minimizing the cutting force [17]:

$$\left[1 - \frac{\sin\beta\sin\phi}{\cos(\beta-\alpha)\cos(\phi-\alpha)}\right]\left[\frac{1}{\cos^2(\phi-\alpha)} - \frac{1}{\sin^2\phi}\right] = \tag{4}$$
$$-\left[\cot\phi + \tan(\phi-\alpha) + Z\right]\left[\frac{\sin\beta}{\cos(\beta-\alpha)}\left(\frac{\cos\phi}{\cos(\phi-\alpha)} + \frac{\sin\phi\sin(\phi-\alpha)}{\cos^2(\phi-\alpha)}\right)\right]$$

where Z=$R/\tau_y t_o$. The friction angle β, in both Merchant's model and Atkins' model, is calculated from the measured values of the cutting force F_c and thrust force F_t in an identical manner as follows.

$$\beta = \tan^{-1}\left(\frac{F_t}{F_c}\right) + \alpha \tag{5}$$

Additionally, the shear strain, γ, is calculated as $\cot\phi + \tan(\phi-\alpha)$ in both Atkins' and Merchant's model. Atkins [17, 18] has provided an elaborate procedure for calculating R and τ_y to fit the machining model to experimental data (see Fig. 7). This method is an iterative procedure of guessing values of

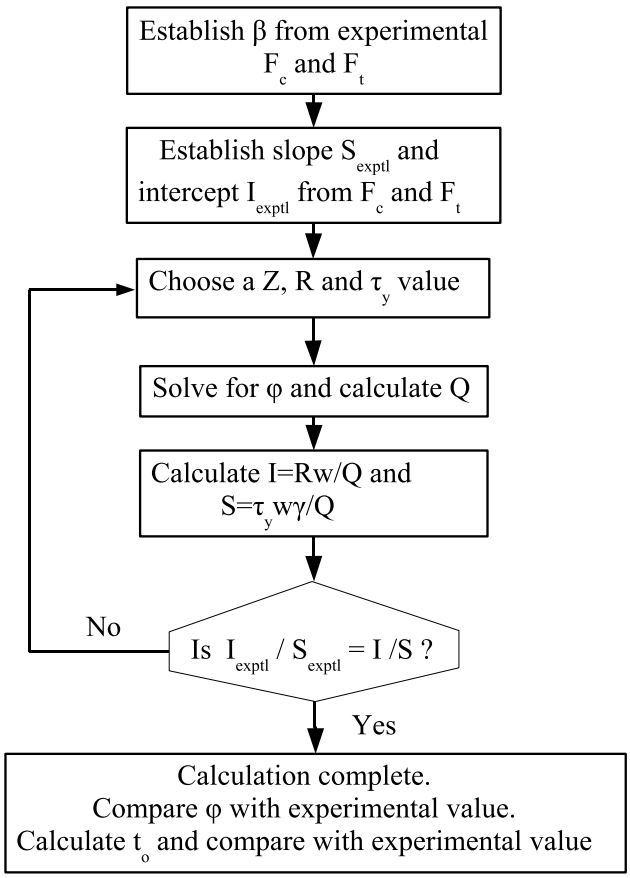

Fig. 7. Flow chart depicting Atkins model calculations: Note that ϕ is calculated from Eqn. 4

R and τ_y until a proper match to the experimental force curve (intercept and slope) is obtained. Since this procedure is little different from a regression fit,

a least square fit method is adopted in this work. With R, and τ_y as parameters, the model is fitted to the data using least squares minimization of the measured and modeled cutting forces. The resulting fit is shown in Figure 8. This fit was obtained for $R = 5.4 \times 10^3$ J/m^2 and $\tau_y = 148.0$ MPa. The values

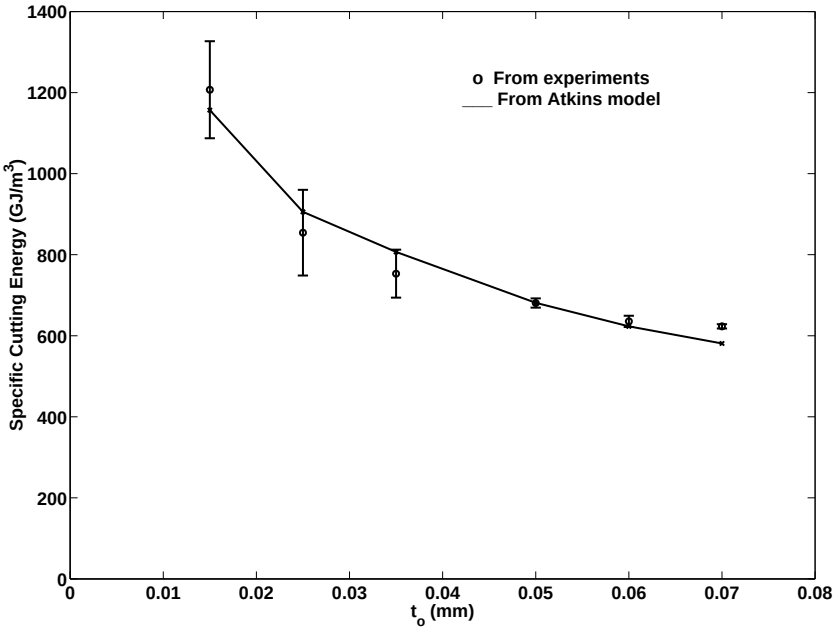

Fig. 8. Specific cutting energy variation with uncut chip thickness (measured and predicted)

of specific energy in shear, friction and material separation (calculated from Atkins model, Eqn. 1) are given in Table 4. It can be seen that while the

Table 4
Specific Energies from Atkins Model

t_o (μm)	U (GJ/m^3)	U_{shear} (GJ/m^3)	$U_{friction}$ (GJ/m^3)	$U_{separation}$ (GJ/m^3)
15	1157.73	373.82	0.47	0.36
25	905.80	323.25	0.36	0.22
35	806.83	297.66	0.33	0.15
50	681.30	267.93	0.29	0.11
60	623.25	254.74	0.27	0.09
70	580.95	249.27	0.27	0.08

specific energy of shear is highest, the specific energy in material separation is comparable to that of friction particularly at small values of t_o. Hence, neglecting this component of energy can cause substantial error in the machining

model when applied to micro-cutting.

The shear angle values calculated from the Atkins model (Eq. 4) were then compared to those obtained by measurements of the chip thickness t_c (Eq. 2), along with those obtained by Merchant's model (Eq. 3). The graph comparing this comparison is shown in Figure 9. It can be seen that the Atkins model

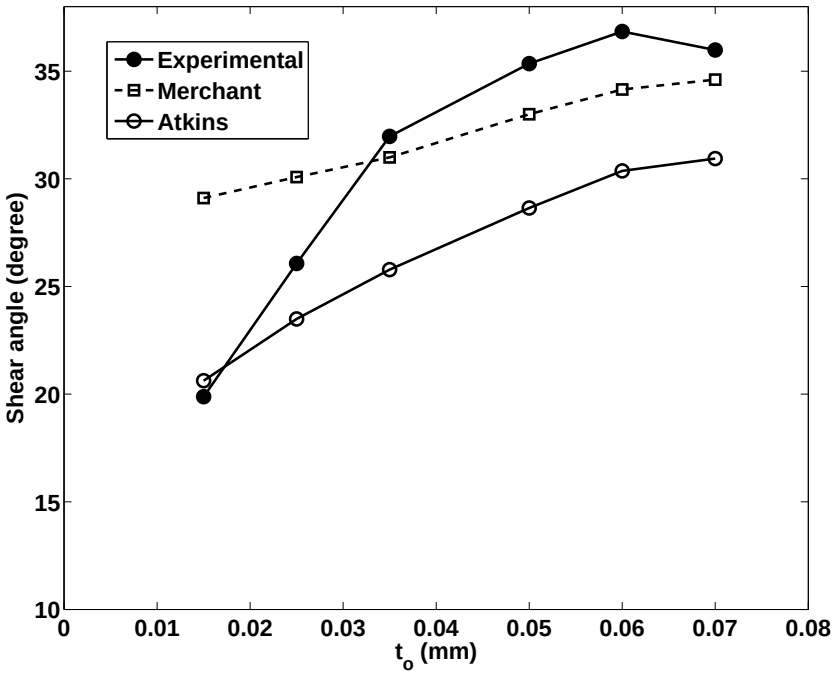

Fig. 9. Shear angle (ϕ) variation with uncut chip thickness - experimental, Merchant model and Atkins model

predicts the trends in the shear angle better than the Merchant model. The utility of the Atkins model in predicting shear angle is more apparent when comparing shear angle predictions in different work materials since material dependence is captured via the fracture toughness term R, while Merchant's model contains no material dependence in the shear angle expression. The rest of the paper compares the fitted values of R and τ_y to that available in the literature for OFHC Copper.

Assuming a Dugdale type of cohesive zone model for the fracture zone ahead of the tool, the fracture toughness R can be estimated as,

$$R = \frac{1}{2}\frac{K_c^2(1-\nu^2)}{E} \tag{6}$$

The factor of two in the denominator comes in because only one-half of the crack is considered. Using values of $K_c = 56$ MPa$\sqrt{m}$ [21], $E = 124$ GPa

and $\nu = 0.34$ [22], the value of fracture toughness, for OFHC Copper, can be determined as $R = 11.2 \times 10^2$ J/m^2. The fitted value of $R = 5.4 \times 10^2$ J/m^2 and the fracture toughness value are of the same order of magnitude.

The yield stress in shear for OFHC copper can be determined from studying its flow stress curves available in the literature [22]. The flow stress is plotted for different strain rates in Figure 10. It is seen from this figure that the flow

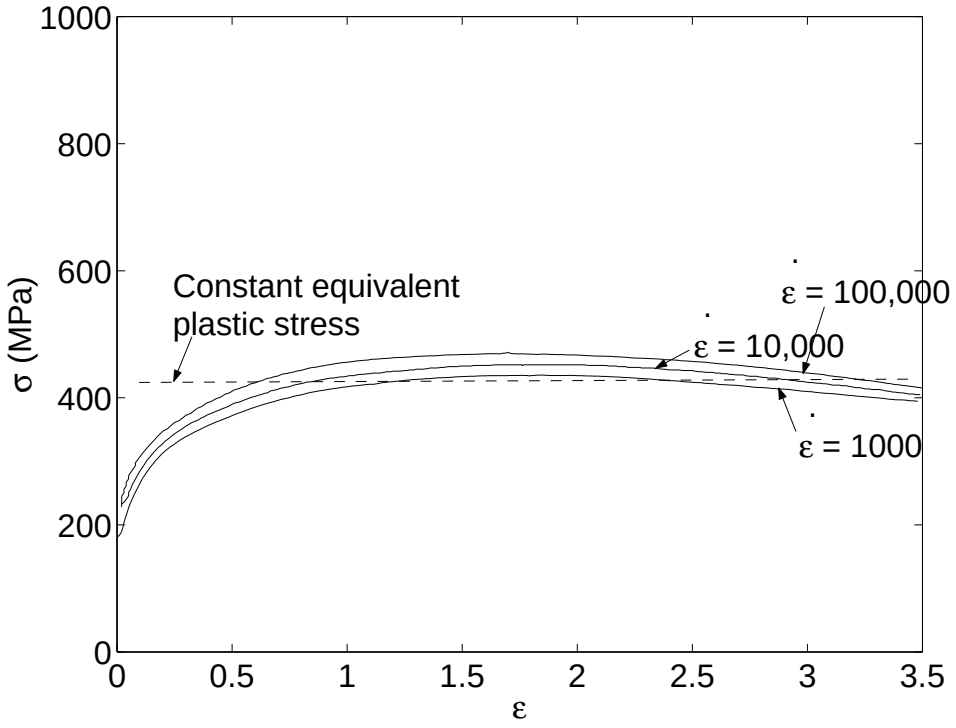

Fig. 10. OFHC Copper flow stress as a function of strain and strain-rate [22]; equivalent plastic yield stress is shown

stress approaches a constant value at higher strains. At strains above 0.5 the material yields without much change in stress, which is constant at about 425 MPa. Also, as shown by the stress-strain curves, the flow stress for OFHC Cu exhibits only a weak dependence on the strain rate at high strains. Hence, at low or high strain-rate the yield stress is relatively unchanged. Using the Tresca yield criterion, the yield stress in shear is then half this value of 212.5 MPa. This is of the same order of magnitude as the fitted value of $\tau_y = 148.0$ MPa. Note that here only an order-of-magnitude comparison is made. The complex nature of stress ahead of the tool may not permit a simple fracture model as assumed. R may not necessarily be constant but vary with strain, strain-rate and temperature. The error can be reduced by introducing more complex fracture models.

The R values obtained by fitting the model to experimental data are average values at best. It is expected that R will change at lower uncut chip thickness

values. The reason for this is as follows. In machining the ductile fracture ahead of the tool is very close to the free surface of the workpiece. At very low uncut chip thickness values, the plastic zone ahead of the crack tip will start to interact with the free surface and the fracture toughness is then expected to change. Investigations in this area are in progress and will be reported in the future.

It is thus seen that the fitted values of the two parameters, fracture toughness and shear yield stress, compare well on an order of magnitude basis. At low cutting speeds where strain-rates and temperature effects are small, the Atkins model of machining appears to explain the trends in machining data and phenomenon fairly well.

6 Summary and Conclusions

In this work, the Atkins model, which incorporates a third term for the energy expended in material separation [17], is evaluated by performing orthogonal cutting tests on OFHC Copper and experimental evidence in the form of SEM pictures depicting ductile tearing ahead of the tool are provided. The main conclusions of this work are:

- The Atkins model of machining, which explicitly includes energy needed for material separation as that due to ductile fracture, can phenomenologically explain effects such as the increase in specific cutting energy with decrease in uncut chip thickness.
- At low cutting speeds where strain-rate and temperature effects are minimal, the Atkins model fits the experimental data fairly well for values of fracture toughness, coefficient of friction and shear yield stress, that are of the same order of magnitude as that reported in the literature.
- Ductile tearing leading to chip formation occurs at uncut chip thickness as low as $25\mu m$.

References

[1] Y. Yamagata, S. Mihara, N. Nishioki, T. Higuchi, A new fabrication method for micro actuators with piezoelectric thin film using cutting technique, Proceedings IEEE Micro-Electro-Mechanical-Systems Feb 11-15, San Diego, CA (1996) 307–311.

[2] M. E. Merchant, Mechanics of the metal cutting process. I. Orthogonal cutting and a Type 2 chip, Journal of Applied Physics 16 (5) (1945) 267–275.

[3] M. C. Shaw, Metal cutting principles, Oxford Science Publications, New York, 1997.
[4] W. R. Backer, E. R. Marshall, M. C. Shaw, The size effect in metal cutting, Transactions of the ASME 74 (1952) 61–72.
[5] E. M. Kopalinsky, P. L. B. Oxley, Size effects in metal removal process, 3rd Conf. Mech. Prop. High Rates of Strain (1984) 389–396.
[6] S. S. Joshi, S. N. Melkote, An explanation for the size-effect in machining using strain gradient plasticity, Proc. JSME/ASME Int. Conf. on Materials and Processing, 1 (2002) 318–323.
[7] N. Fang, Slip-line modeling of machining with a rounded-edge tool - parts I and II, J. Mech. Phy. Solids 51 (2003) 715–762.
[8] M. C. Shaw, The size effect in metal cutting, Sadhana 25 (5) (2003) 875–896.
[9] D. Dinesh, S. Swaminathan, S. Chandrasekhar, T. N. Farris, An intrinsic size-effect in machining due to the strain gradient, Proc. ASME IMECE, New York (2001) 197–204.
[10] K. Liu, S. N. Melkote, A strain-gradient based finite element model for micro-meso scale orthogonal cutting process, Proc. 2004 Japan/USA Symposium on Flexible Automation, Denver, CO, USA.
[11] M. C. Shaw, A quantized theory of strain hardening as applied to cutting of metals, Journal of Applied Physics 21 (1950) 599–606.
[12] K. Nakayama, K. Tamura, Size effect in metal-cutting force, Trans. ASME, Journal of Engineering for Industry (1968) 119–126.
[13] E. G. Thomsen, J. T. Lapsley, R. C. Grassi, Deformation work absorbed by the workpiece during metal cutting, Transactions of ASME 75 (1953) 591–603.
[14] J. A. Arsecularatne, On tool-chip interface stress distributions, ploughing force and size effect in machining, International Journal Machine Tools ad Manufacture 37 (7) (1997) 885–899.
[15] E. J. A. Armarego, R. H. Brown, On the size effect in metal cutting, Int. J. Prod. Res. 1 (1962) 75–99.
[16] A. G. Atkins, Fracture toughness and cutting, International Journal of Production Research 12 (2) (1974) 263–274.
[17] A. G. Atkins, Modelling metal cutting using modern ductile fracture mechanics: quantitative explanations for some longstanding problems, International Journal of Mechanical Sciences 45 (2003) 373–396.
[18] A. G. Atkins, Toughness and Cutting: a new way of simultaneously determining ductile fracture toughness and strength, Engineering Fracture Mechanics 72 (2005) 849–860.
[19] S. Subbiah, S. N. Melkote, The constant force component due to material separation and its contribution to the size-effect in specific cutting energy, ASME Transactions J. Manuf. Sci. Engg 128 (3) (2006) 811–815.
[20] S. Subbiah, S. N. Melkote, On the size effect in micro-cutting at low and high rake angles, Proceedings of ASME IMECE, Anaheim, CA, November 13-15, MED MED-15 (2004) 485–493.

[21] A. Nyilas, A. Nishimura, B. Obst, Further aspects on J-evaluation demonstrated with EDM notched round bars and double-edged plates between 300 and 7 K, Proc. of Int. Cryogenic Materials Conf ICMC 48 (2002) 131–138.
[22] G. R. Johnson, W. H. Cook, Fracture characteristics of three metals subjected to various strains, strain rates, temperatures and pressures, Engineering Fracture Mechanics 21 (1) (1985) 31–49.
[23] L. Engel, H. Klingele, An Atlas of Metal Damage, Page 41, Prentice-Hall, Inc., New Jersey, 1981.